

Geophysical Research Letters®

RESEARCH LETTER

10.1029/2022GL099586

YuRui Li, Yang Zhang contributed equally to this work.

Key Points:

- The spatial distribution of fractal dimension (FD) is obtained, and used to describe lightning channel morphology
- The channel morphology characterized by the FD is closely related to channel development velocity and radiation power density
- The channel morphology can be used to reflect the inhomogeneous state of charge level distribution

Supporting Information:

Supporting Information may be found in the online version of this article.

Correspondence to:

Y. Zhang and Y. Zhang,
zhangyang@cma.gov.cn;
zhangyijun@fudan.edu.cn

Citation:

Li, Y., Zhang, Y., Zhang, Y., & Krehbiel, P. R. (2022). Analysis of the configuration relationship between the morphological characteristics of lightning channels and the charge structure based on the localization of VHF radiation sources. *Geophysical Research Letters*, 49, e2022GL099586. <https://doi.org/10.1029/2022GL099586>

Received 14 MAY 2022

Accepted 8 JUL 2022

Analysis of the Configuration Relationship Between the Morphological Characteristics of Lightning Channels and the Charge Structure Based on the Localization of VHF Radiation Sources

YuRui Li^{1,2}, Yang Zhang² , YiJun Zhang^{1,3,4}, and Paul R. Krehbiel⁵ 

¹Department of Atmospheric and Oceanic Sciences and Institute of Atmospheric Sciences, Fudan University, Shanghai, China, ²State Key Laboratory of Severe Weather, Chinese Academy of Meteorological Sciences, Beijing, China, ³CMA-FDU Joint Laboratory of Marine Meteorology and Shanghai Frontiers Science Center of Atmosphere-Ocean Interaction, Shanghai, China, ⁴Shanghai Qi Zhi Institute, Shanghai, China, ⁵Langmuir Laboratory for Atmospheric Research, Geophysical Research Center, New Mexico Institute of Mining and Technology, Socorro, NM, USA

Abstract The lightning channel morphology is closely related to developmental processes, which depends on the charge structure. There is currently a lack of understanding of how lightning channel morphology reveals developmental characteristics and charge structure. Based on the Lightning mapping array radiation source localization data of six lightning flashes, we studied the lightning channel morphology characterization method and obtained the spatial distribution of the fractal dimension (FD). We found that the fractal distribution had a consistent spatial and temporal correspondence with the channel development characteristics. Compared to regions with unidirectional extended channels, regions with more channel branches or direction change of channel development have a larger FD and a higher power density, where horizontal channel development is accelerated. These correspondence features reflect the inhomogeneous presence of pocket charge, which provides a new method to use lightning morphology information to reveal the characteristics of charge level distribution within thunderstorm clouds.

Plain Language Summary The charge distribution within the horizontal charge region may have a more significant effect on the extension of the lightning channel. At present, it is still difficult to directly observe the charge structure of thunderstorm clouds, especially the horizontal charge structure. Also, the morphological study of the channel is not perfect due to the limitations of observation and data acquisition. Therefore, there is currently a lack of understanding of how lightning channel morphology reveals developmental characteristics and charge structure. In the paper, the relationship between the lightning channel morphology, developmental characteristics, and charge structure was investigated for the first time based on Lightning mapping array localization data, and the spatial distribution of the lightning fractal dimension (FD) was obtained. It is found that, compared to regions with unidirectional extended channels, regions with more channel branches or direction change of channel development have a larger FD and a higher power density, where horizontal channel development is accelerated. These correspondence features reflect the inhomogeneous presence of pocket charge, which provides a new method to use lightning morphology information to reveal the characteristics of charge level distribution within thunderstorm clouds.

1. Introduction

The spatial distribution of charge plays a crucial role during lightning development (Iudin et al., 2017; Zheng et al., 2019). A typical thunderstorm cloud has a three-layer charge structure: a positive charge region at the top, a negative charge region in the middle and a small positive charge region at the bottom (Krehbiel, 1986; Williams et al., 1985). At present, the vertical layered structure is mainly used in research to reveal the propagation behavior of lightning (Krehbiel, 2003; Nag & Rakov, 2009; Qie, 2005). However, a growing body of research suggests that the charge structure of thunderstorm clouds is more complex (Stolzenburg et al., 1998) and possibly manifests itself as a staggering of more charge regions, and the horizontal extent of the charge regions can often be much larger than the vertical extent (Coleman et al., 2003; Krehbiel et al., 1979; Lyons et al., 2020; MacGorman et al., 1981; Winn et al., 1981). The nonuniformity of the charge distribution within the horizontal charge region may have a more significant effect on the extension of the lightning channel.

At present, channel development is generally simulated by assuming the charge distribution in the numerical model, and the correctness of the assumption of the charge structure is proved by the development and transport characteristics obtained by the simulation (Mansell et al., 2002; Niemeyer et al., 1984). For example, Tan et al. (2014) proposed a horizontal larger charge region effect through two-dimensional simulations, which suggests that the polarity and type of lightning discharge depend on the relative position and size of the charge region near the initiation point. Xu et al. (2021) presented similar conclusions to Tan et al. (2014) by simulating different horizontal charge distribution characteristics, which revealed the influence of the uniformity of the horizontal charge distribution and relative position of high-density charge centers on the propagation trend of the leader and type of lightning. Iudin et al. (2017) showed through simulations that the occurrence of different types of lightning depended on the charge structure. However, numerical models are based on certain speculations and assumptions, and the reality of the results must be tested by actual detection results.

The actual detection of the charge region within a thunderstorm cloud consists of two main approaches: electric field sounding and radiation source-based inversion. The electric field sounding information can only obtain the field intensity distribution along the balloon's ascending trajectory in a certain time range and cannot obtain the instantaneous potential and charge spatial distribution in the cloud. It is still difficult to understand the interrelationship between the channel development of the discharge process and the charge spatial distribution in the cloud. The radiation source-based inversion method of charge distribution is usually based on the understanding of the lightning discharge process and radiation laws. However, considering the insufficient details of channel development, only a typical layered structure in the discharge was given (Krehbiel, 1986). The radiation source localization results, especially the channel morphology information, can characterize the channel extensions, which are closely related to the charge structure; thus, they are expected to reflect more detailed charge structure characteristics through channel morphology and development characteristics studies. Previous laboratory-based experimental and numerical simulation studies have also shown the feasibility of this method. For example, Williams et al. (1985) and Mansell et al. (2002) demonstrated experimentally and through simulations that electrical discharges tended to propagate more into regions of higher charge density, where there was more abundant branching and the abundant bifurcation could manifest itself in larger fractal dimensions. Tan et al. (2007) found that the propagation of cloud-to-cloud flash was related to the distribution of charges in clouds through numerical model simulations, and the leader propagated first to the high-density centers and potential extremes.

The morphological study of the channel is not perfect due to the limitations of observation and data acquisition. In the past, although there were studies on the description of lightning using fractals based on measured data, they mainly used the fractal dimension (FD) of waveforms to distinguish different lightning categories (Gou et al., 2010) or fractal dimensions to describe the geometric characteristics of each lightning as a whole. However, they did not describe the spatial distribution of fractals in a single lightning flash and failed to characterize the developmental changes in channels by fractal dimensions (Sañudo et al., 1995; Tan et al., 2006). In this study, we obtain lightning development channels from radiation source localization data, perform FD characterization to investigate the relationship among the FD, channel morphology and power density, and explore the role of lightning channel morphological characteristics on the indication of charge area.

2. Data and Methods

2.1. Data

This study focuses on the analysis of 3D location data from radiation sources of six lightning flashes during a thunderstorm in New Mexico, USA, on 5 August 2013. The location data were obtained from the Lightning mapping array (LMA) observations at the Langmuir Laboratory of the New Mexico Institute of Mining and Technology (NMT). The 3D location has a temporal resolution of 80 μ s and a location accuracy of tens of meters within the network of stations (Rison et al., 1999; Thomas et al., 2004). A strict standard of noise reduction is used (number of stations ≥ 7 ; reduced chi-square ≤ 2) to ensure the reliability of the location data. Six flashes occurred on 5 August 2015, at 20:01:16, 20:02:56, 20:04:10, 20:05:13, 20:10:01 and 20:27:08 UTC (later referred to as flash one, flash two, flash three, flash four, flash five and flash six, see Table S1 in Supporting Information S1 for more details), and the occurrence location was concentrated in the range of 12 km from east to west and 20 km from north to south, with high positioning accuracy. The three-dimensional localization distribution is shown in Figure S1 of Supporting Information S1. The main text focuses on flash two as an example to illustrate the findings of this study and the distribution of flash two is shown in Figure 1a. The KABX radar in Albuquerque, New Mexico,

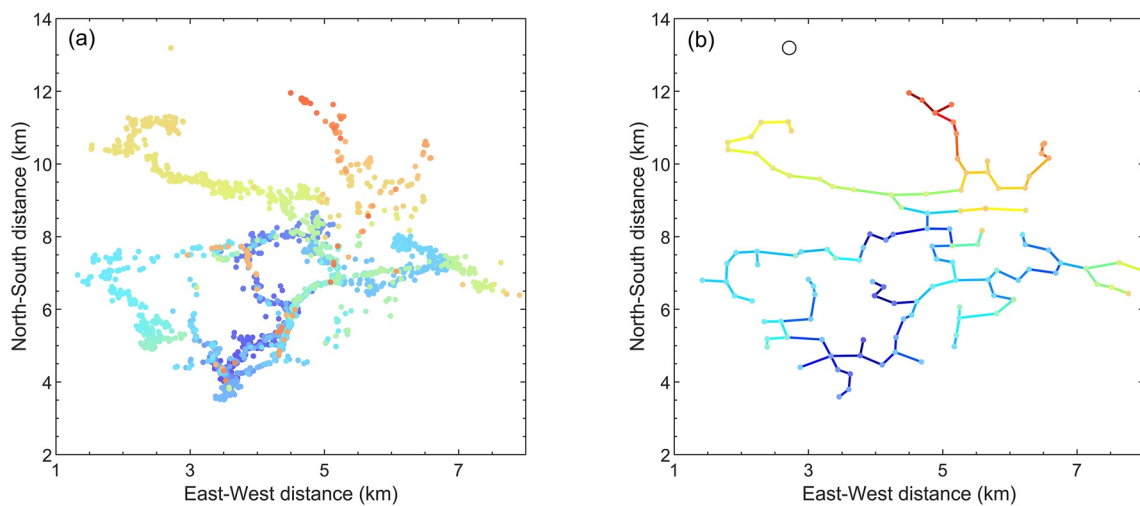


Figure 1. (a) Horizontal projection of Flash two; (b) Flash two channel fit (0.50×0.50 km grid points). The radiation sources are colored by time.

located approximately 130 km east-northwest of the center of the LMA, provided the base data, and the lightning flashes analyzed here are all about 125 km away from the radar and within the radar detection range.

2.2. Calculation of Fractal Dimension

Fractal is a natural framework to describe chaos and complex structures (Barnsley & Jacquin, 1988) and has been successfully applied to geometrically describe electrical discharges (Femia et al., 1993). The geometry of lightning is fractal (Riousset et al., 2007; Vecchi et al., 1994), and the use of fractal dimensions enables a quantitative description of the morphology of lightning channels, such as the direct extension, steering, and bifurcation behavior of lightning channels. In this paper, the FD is used to characterize the channel morphology, and the box-counting method is used to calculate the FD (see Maragos and Sun (1993) for details) as follows:

$$FD = \lim_{\varepsilon \rightarrow 0} \frac{\log N(\varepsilon)}{\log \frac{1}{\varepsilon}}$$

where ε is the side length of the box, and N is the number of boxes covered. In the specific calculation process, the radiation source is first approximated to fit to obtain a stable FD. The method is similar to Zhang et al. (2014), where the analysis space is divided into a grid of 0.50×0.50 km, and the arithmetic average of all radiation source positions within each grid point is taken as the average position of the radiation source within this grid point. Then, the channels are fitted by interpolation between the radiation sources obtained in the previous step according to the lightning channel connection method (Li et al., 2021). The shape of the fitted channels is shown in Figure 1b. When the number of interpolations is 11, it is approximately the same as the original data (Figure 1a), the FD tends to be stable, and the number of radiation sources is close to the number before fitting. Finally, the FD of each grid point is calculated to obtain the FD distribution of the area to be analyzed.

2.3. Estimation Method and Fitting of the Leader Velocity

The leader velocity was calculated in a similar manner to Jensen et al. (2021). The radiation sources of the leader channel were selected, and the velocity of the leader propagation was estimated using the sliding average method (see Text S1 in Supporting Information S1 for more details). A velocity estimate was obtained at each sliding window, and the curve of velocity variation with time can be obtained after sliding through the window. Figure S2 in Supporting Information S1 shows the results of fitting a section of leader radiation sources in Flash two with different sliding steps (10 sources, 40 sources, 70 sources) and the calculated velocities. When taking a sliding step of 40 radiation sources, the fitted channel can match the radiation source morphology, and the velocity changes are more continuous.

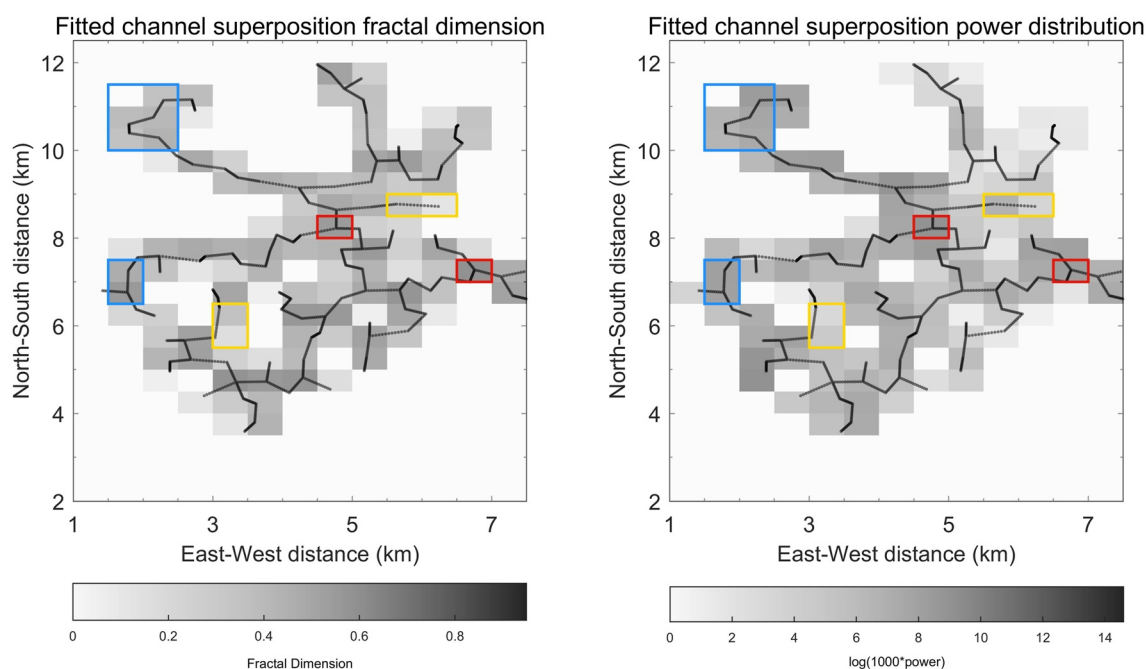


Figure 2. (a) Channel morphology superimposed on the fractal dimension (FD), and (b) channel morphology superimposed on the power density distribution. The black line represents the fitted channel; the grayscale plot represents the FD distribution; the blue box indicates the inflection point location; the red box indicates the bifurcation location; the yellow box indicates the channel one-way extension region.

3. Result

3.1. Channel Morphology and Fractal Characteristics

The effects of the channel curvature and number of branches on the FD in the ideal case are first explored. In contrast to a previous study of the fractal characteristics of each lightning event as a whole (Allen et al., 2011; Tsonis, 1991), Figures S3a–S3d in Supporting Information S1 show the change in FD for simulated channels with different degrees of curvature within a 0.5×0.5 km grid point. With the increase in inflection points, the FD also increases. Figure S3e–S3h in Supporting Information S1 shows the change in FD with a given number of branches within a 0.5×0.5 km grid. The FD increases with the increase in number of branches. From the above ideal simulation, the size of the FD truly reflects the tortuosity of the lightning channel and the number of branches.

Figure 2a shows the channel FD distribution of the observed lightning Flash two. The yellow boxes ($(N, E) = (5.5-6.5, 3-3.5)$ km and $(N, E) = (8.5-9, 5.5-6.5)$ km) are the regions of direct lightning extension with fractal dimensions of 0.5026 and 0.4344, respectively, and a mean value of 0.4685. Near the blue boxes ($(N, E) = 10-11.5, 1.5-2.5$ km and $(N, E) = (6.5-7.5, 1.5-2)$ km) are the regions where the channel propagation direction changes (inflection points, which are also another manifestation of branching) with fractal dimensions of 0.8426 and 0.6812, respectively, and an average of 0.7619. Near the red boxes ($(N, E) = 8-8.5, 4.5-5$ km and $(N, E) = (7-7.5, 6.5-7)$ km) are the regions of channel branching with fractal dimensions of 0.8834 and 0.9560, respectively, with an average of 0.9197. The magnitude of the FD directly characterizes the morphology of the lightning channel: the largest FD is where the channel bifurcates, and the smallest FD is in the region of unidirectional development. In contrast, the FD values obtained in previous studies are for the whole lightning, for example, 4/3 for Tsonis (1991) based on lightning photographs and 5/3 for the whole lightning obtained by Allen et al. (2011) based on LMA, which give fractal characteristics that describe the lightning as a whole and cannot describe the lightning details. We use the spatial distribution of fractal dimensions to characterize the developmental morphology of the channel in the following study.

3.2. Lightning Channel Morphology and Power Density Distribution

We define the power density as the sum of the power of all Very High Frequency (VHF) radiation sources in a unit area, which is used to represent the comprehensive effect of the number and power of the radiation sources and reflects the discharge energy per unit area. We analyze the relationship between lightning channel morphology and power density for the same region as the channel morphology and FD in Section 3.1. Figure 2b shows the superposition of the fitted lightning channel morphology and VHF power density. The power density of the VHF radiation sources is 89.92 and 7.91, with an average of 48.92 W/km^2 near the yellow box in the figure, where the lightning extends in one direction. Near the blue box is the inflection point of the channel, and the power densities of the VHF source are 1,141.79 and 566.41 with an average of 854.10 W/km^2 ; Near the red box are the branching areas with VHF source power densities of 7,341.09 and 3,120.04 and an average of $5,230.57 \text{ W/km}^2$. Combined with the FD characteristics of the corresponding regions in Section 3.1, the unidirectional extension of the channel has the smallest power density and the smallest corresponding FD, while the branch has the largest power density and the largest corresponding FD.

3.3. Channel Morphology and Leader Velocity

We selected the leaders that continuously developed within the height of 9–11 km in the time period of 20:02:57.10–20:02:56.17 (Figure 3a) and analyzed the relationship between the leader propagation velocity and the channel morphology. As shown in Figure 3, the leader propagates towards region A at a velocity of approximately $0.5 \times 10^5 \text{ m/s}$, and the velocity increases to more than $2 \times 10^5 \text{ m/s}$ at region A, which is 4 times the starting velocity. As seen in Figures 3b, 3e and 3f, region A is the region of channel bifurcation, where it has large FD and power density (1.0920 and $1,872.03 \text{ W/km}^2$, respectively). Then, the leader continues to propagate towards the northwest direction without obvious bifurcation and big direction change, the FD and power density are small, and the velocity is approximately $0.5 \times 10^5 \text{ m/s}$. Near region B, the leader velocity increases to 3 times the usual velocity, approximately $1.5 \times 10^5 \text{ m/s}$. After that, the velocity decreases and subsequently rapidly increases in the process of propagation to region C, and the velocity is approximately $1.25 \times 10^5 \text{ m/s}$ at the region C, which is 2.5 times the usual. In Figures 3e and 3f, regions B and C are in the channel inflection point and development direction change region, respectively, with large fractal dimensions and power densities of 1.0371 and 796.254 W/km^2 for region B and 1.1004 and $1,132.82 \text{ W/km}^2$ for region C. The FD and power density of region C are 1.1004 and $1,132.82 \text{ W/km}^2$, respectively. The average FD and power density of the one-way development area of the channel between A and B are 0.7584 and 597.3674 W/km^2 . This analysis shows that the leader transport accelerates in regions with large fractal dimensions and large power densities.

3.4. Channel Morphology and Charge Structure

The analysis in 3.1–3.3 shows that the FD can reflect the characteristics of channel morphology (number and tortuosity of branches), power density of radiation sources, and channel development velocity. The FD is larger and the power density is higher at the rich branches (change of development direction), and the leader transmission is accelerated in the region with a large FD. Theoretically, the changing laws of these morphologies and discharge characteristics are related to the charge structure. We believe that in the layered charge region of thunderstorm clouds, there is a certain inhomogeneity in the distribution of charges, there are certain pocket charges, which enhance the local electric potential, and the surrounding electric field is relatively strong. Strong electric fields will lead to more breakdown discharges, which results in more and stronger radiation sources and a greater discharge power density. The leader development is also faster under a strong electric field. According to the relationship between channel morphology and power density and leader velocity derived from the analysis in this paper, the region with the pocket charge is likely the region where the channel branches and turns. We speculate from the analyzed cases in this paper, the horizontal distribution of charges is not uniform, and the charge density is greater in regions with large fractal dimensions. Similar to our conjecture, previous laboratory experiments and simulations have suggested that the discharge tends to propagate more into the region of higher charge density, where there is more abundant branching, and the discharge propagation velocity increases with increasing charge density (Mansell et al., 2002; Williams et al., 1985). Furthermore, Scholten et al. (2021) found the case of leader acceleration, and they proposed that the sudden increase in leader velocity might be attracted by a strong electric field region called pocket charge. Stock et al. (2017) found that the increase in leader velocity was also accompanied by a sudden increase in VHF power when a fast positive breakdown event occurred, which generally

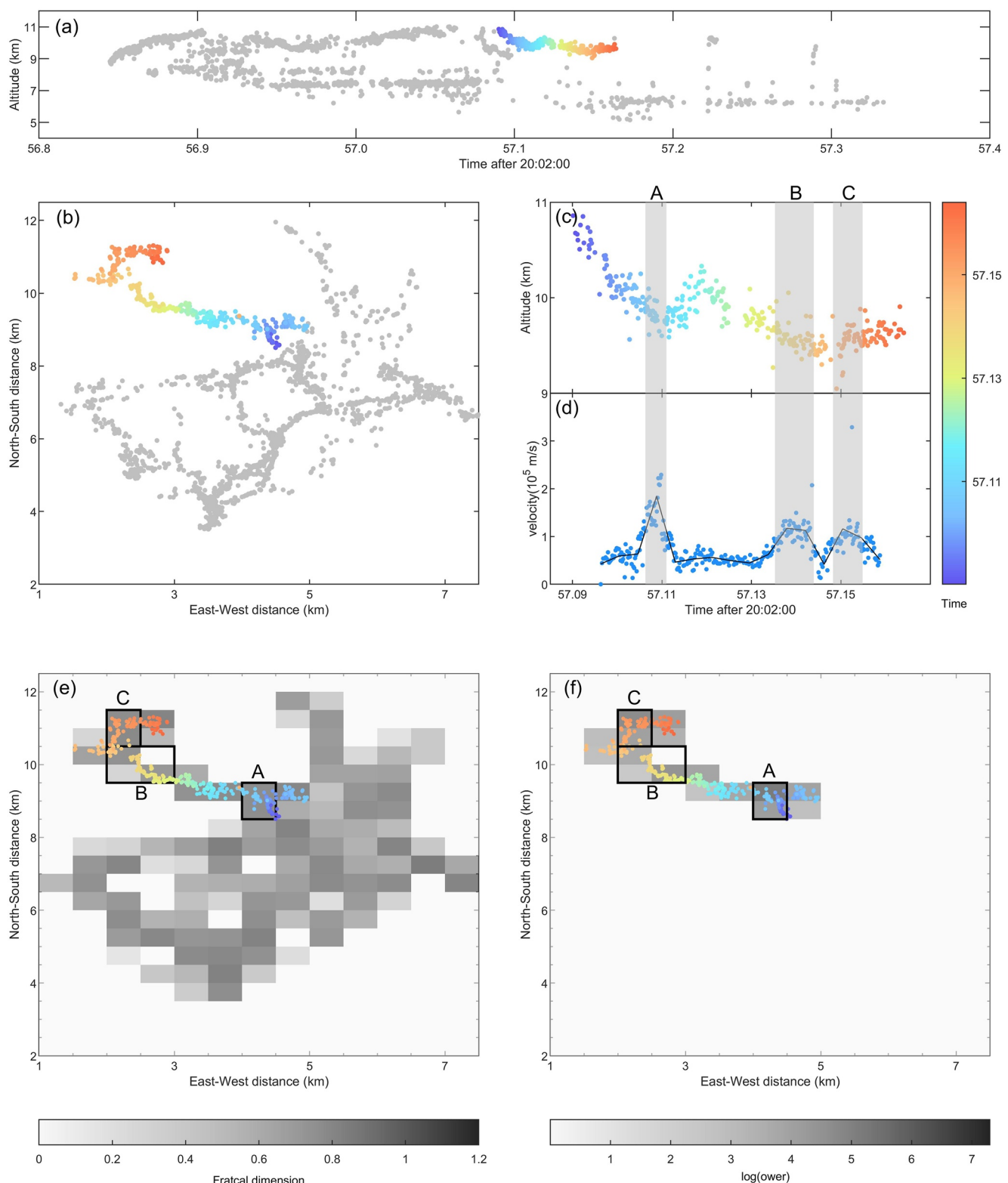


Figure 3. (a) Time-height plot of flash one; (b) planar projection of flash one; (c) local magnification of the colored part of Figure (a); (d) leader velocity variation with time; (e) fractal dimension (FD) of the VHF radiation source superimposed on the 0.25×0.25 km fitted channel; (f) VHF radiation source superimposed on the power density distribution. The gray dots indicate the distribution of the whole flash, the colored dots indicate the analyzed region, and the grayscale plots indicate the FD distribution and power density distribution.

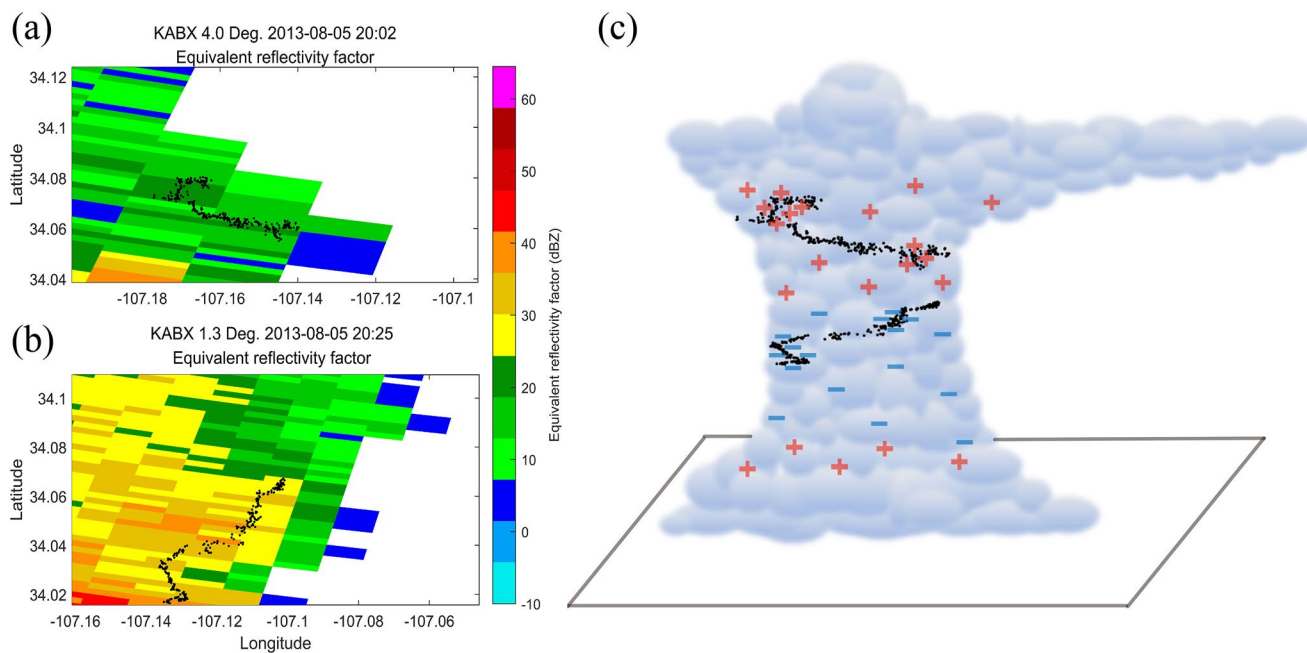


Figure 4. (a) VHF radiation source of flash two superimposed on the reflectivity Plan Position Indicator (PPI) of KABX radar with 4° elevation angle; (b) VHF radiation source of flash 6 superimposed on the reflectivity PPI of KABX radar with 1.3° elevation angle. The shading is the radar equivalent reflectivity factor, and the black dots represent the VHF radiation sources. (c) Conceptual model of thunderstorm cloud charge structure and lightning channel morphology. The red + and blue - represent the positive and negative charge regions, respectively; the dense symbols (+ and -) represent the regions of high charge density, that is, pocket charge; the black dots indicate the Lightning mapping array radiation sources.

occurs in the region of strong electric fields. Cooke et al. (1982) measured the effect of the charge density on the propagation velocity in the laboratory using polymethylmethacrylate, and they showed that the velocity sharply increased with increasing space charge density.

We also verified the other five cases (see Table S2 in Supporting Information S1 for detailed data and analysis) and statistically analyzed the FD, power density, and leader velocity characteristics of the directly extended region and the bifurcation or transmission direction change region. All cases showed the inhomogeneity of the FD distribution, power density and leader velocity in the discharge region. Since our analysis is mainly aimed at horizontal transport within the charge layer, these inhomogeneous distributions can be used to qualitatively describe the inhomogeneous distribution of horizontal charge in thunderstorm clouds. Based on the results of this paper, a conceptual model of charge structure and lightning channel morphology in thunderstorm cloud is given. As shown in Figure 4c, the red + and blue - represent the positive and negative charge layers in a typical thunderstorm, respectively; the dense symbols (+ and -) indicate the regions of high charge density, that is, pocket charge; the black dots represent the VHF radiation sources. The location of lightning bifurcation and turning is precisely the region with high radiation source density, high charge density and high discharge power density, which exhibits a large FD in morphological characteristics. The above morphological features describe the inhomogeneity of the horizontal charge structure, which leads to different velocities (Mazur & Rust, 1983) and various channel morphologies during the leader development. In addition, lightning channel morphology and radar reflectivity also have a certain corresponding relationship. Take flash two and flash six as examples, as shown in Figures 4a and 4b, at the altitude of the horizontal development of the lightning channel analyzed in this paper, there is a large radar reflectivity in the channel turning and bifurcation regions, which to a certain extent also indicates that the particle number concentration and charge density are large here.

4. Conclusion and Discussion

Based on LMA localization data of six flashes during a thunderstorm in New Mexico on 5 August 2013, the relationship of the channel morphology, developmental characteristics, and charge structure was investigated for the first time based on the measured data, and the spatial distribution of the lightning FD was obtained. The

characterization method of channel morphology was studied, the FD was used to describe the fine morphology of the lightning, and the relationship between the FD distribution, power density, and leader development velocity was obtained. The findings obtained are as follows:

1. The FD, channel morphology and radiation characteristics are closely related. The region with more branches and development direction change has a larger FD, while the one-way extension region of the channel has a smaller FD. The region with a large FD corresponds to the region of large power density, and the region with a small FD corresponds to the area of small power density.
2. There is a correlation between the channel morphology characterized by the FD and the velocity of leader development. As the leader develops in the horizontal charge region, it accelerates in the region of larger FD and power density, reaching 2.5–4 times the starting velocity in the shown case. The leader at regions of small FD and power density propagates at a smaller velocity.
3. Regions with larger fractal dimensions, power densities and channel development velocities may correspond to local strong electric field regions, which also reveal regions with high charge densities. There is likely a pocket charge at the position of morphological bifurcation and turning, which provides a new method to use lightning morphological information to reveal the horizontal charge structure of thunderstorm clouds.

At present, it is difficult to directly observe the charge structure of thunderstorm clouds, especially the horizontal charge structure. Holmes et al. (1980) and Mazur and Rust (1983) demonstrated the possibility of using radar to monitor the plasma progress of lightning discharges, which provides a valuable means of studying space charge density, but the low temporal resolution of radar can greatly reduce the measurement accuracy. Petersen et al. (2008) and Kostinskiy et al. (2015) speculated that although there were local strong electric fields, they were too local to be easily observed. Mareev and Dementyeva (2017) proposed that charge pockets might be caused by local turbulence. Scholten et al. (2021) speculated the existence of pocket charge regions by observing changes in the leader velocity. Although they strongly indicate the existence of strong electric field regions for the first time, the regions are large and cannot be linked to the intuitive characteristics of lightning morphology. In contrast, based on radiation source localization data of LMA with thunderstorm nonmissing detection capability, our method provides a more general method to reveal the charge structure through channel morphology distribution, extend the application of LMA radiation source localization information and provide new ideas for a deeper understanding of charge structures in the future.

At the height of the horizontal development of lightning, the regions of channel steering and bifurcation correspond to a relatively large radar reflectivity, but the regions of large reflectivity are not necessarily the locations of lightning channel steering and bifurcation. To some extent, the lightning channel morphology in this paper reflects a transient thunderstorm charge structure, which often changes rapidly due to turbulence. However, the low time resolution (6 min) of the weather radar used in this paper makes it difficult to accurately respond to these transients and rapid changes. We will combine with phased-array radars with a higher temporal resolution for a more in-depth comprehensive analysis.

This study only focuses on the two-dimensional morphology of the horizontal charge region, and the charge distribution revealed by the channel morphology in the vertical direction is not considered. In the future, the relationship between the three-dimensional channel morphology and the charge structure can be investigated to reveal the spatial charge density distribution of the entire thunderstorm cloud. In addition, the charge structures revealed by numerical simulations and laboratory experiments are consistent with our results, but these results must be verified by actual in situ sounding data, and it is currently difficult to observe the inhomogeneous distribution of charges in the horizontal direction. The conventional electric field sounders are carried by a sounding balloon, the detection paths are difficult to determine, and the horizontal motion of the sounders in the layered charge region is greatly constrained due to the updraft. This problem may be avoided in the future by using aircraft to carry electric field sounding through clouds to obtain the electric field distribution in the layered charge region and verify the charge structure that we have revealed.

Data Availability Statement

This work complies with the AGU data policy; the data used in this paper can be obtained from the website: <https://doi.org/10.5281/zenodo.6548297>. And the radar data can be obtained from the website: https://www.roc.noaa.gov/WSR88D/Level_II/Level2Info.aspx.

Acknowledgments

This research was funded by the National Natural Science Foundation of China (42175090), the National Key Research and Development Program of China (2017YFC1501501, 2019YFC1510103), the National Natural Science Foundation of China (41775009, and 41905004), and the Basic Research Fund of Chinese Academy of Meteorological Sciences (Grant 2021Z011). The authors are very grateful to the lightning team of NMT for providing LMA data. And also thank the Radar Operations Center of NOAA's National Weather Service which shares the radar data of New Mexico.

References

Allen, B. J., Mansell, E. R., & Bruning, E. C. (2011). Fractal characteristics of simulated and LMA-observed lightning flashes. *Journal of Geophysical Research: Atmospheres*, 116, 1–10. <https://doi.org/10.1029/2010JD014402>

Barnsley, M. F., & Jacquin, A. E. (1988). Application of recurrent iterated function systems to images. In *Proceedings of the SPIE 1001, visual communications and image processing* (Vol. 88). SPIE. *Third in a series*.

Coleman, L. M., Marshall, T. C., Stolzenburg, M., Hamlin, T., Krehbiel, P. R., Rison, W., & Thomas, R. J. (2003). Effects of charge and electrostatic potential on lightning propagation. *Journal of Geophysical Research*, 108, 4298. <https://doi.org/10.1029/2002JD002718>

Cooke, C. M., Williams, E., & Wright, K. A. (1982). Electrical discharge propagation in space-charged PMMA. In *1982 IEEE international conference on electrical insulation* (pp. 95–101). IEEE.

Femia, N., Niemeyer, L., & Tucci, V. (1993). Fractal characteristics of electrical discharges: Experiments and simulation. *Journal of Physics D: Applied Physics*, 26(4), 619–627. <https://doi.org/10.1088/0022-3727/26/4/014>

Gou, X., Chen, M., Du, Y., & Dong, W. (2010). Fractal dynamics analysis of the VHF radiation pulses during initial breakdown process of lightning. *Geophysical Research Letters*, 37(11), L11808. <https://doi.org/10.1029/2010GL043178>

Holmes, C. R., Szymanski, E. W., Szymanski, S. J., & Moore, C. (1980). Radar and acoustic study of lightning. *Journal of Geophysical Research*, 85(NC12), 7517–7532. <https://doi.org/10.1029/JC085iC12p07517>

Iudin, D. I., Rakov, V. A., Mareev, E. A., Iudin, F. D., Syssoev, A. A., & Davydenko, S. S. (2017). Advanced numerical model of lightning development: Application to studying the role of LPCR in determining lightning type. *Journal of Geophysical Research: Atmospheres*, 122, 6416–6430. <https://doi.org/10.1002/2016JD026261>

Jensen, D. P., Sonnenfeld, R. G., Stanley, M. A., Edens, H. E., da Silva, C. L., & Krehbiel, P. R. (2021). Dart-leader and k-leader velocity from initiation site to termination time-resolved with 3d interferometry. *Journal of Geophysical Research: Atmospheres*, 126, e2020JD034309. <https://doi.org/10.1029/2020jd034309>

Kostinskiy, A. Y., Syssoev, V. S., Bogatov, N. A., Mareev, E. A., Rakov, V. A., Makalsky, L. M., et al. (2015). Infrared images of bidirectional leaders produced by the cloud of charged water droplets. *Journal of Geophysical Research: Atmospheres*, 120, 10728–10735. <https://doi.org/10.1002/2015JD023827>

Krehbiel, P. R. (1986). The electrical structure of thunderstorms. In E. P. Krider & R. G. Roble (Eds.), *The Earth's electrical environment* (pp. 90–113). National Academy Press.

Krehbiel, P. R. (2003). Thunderstorm observations with the lightning mapping array. In *Proceedings of the 12th international conference on atmospheric electricity*.

Krehbiel, P. R., Brook, M., & McCrory, R. A. (1979). An analysis of the charge structure of lightning discharges to ground. *Journal of Geophysical Research*, 84(C5), 2432–2456. <https://doi.org/10.1029/JC084iC05p02432>

Li, Y. R., Zhang, Y., Zhang, Y. J., & Krehbiel, P. R. (2021). A new method for connecting the radiation sources of lightning discharge extension channels. *Earth and Space Science*, 8(7), e2021EA001713. <https://doi.org/10.1029/2021ea001713>

Lyons, W. A., Bruning, E. C., Warner, A., Macgorman, D. R., Mlynarczyk, J., & Tillier, C. (2020). MEGAFLASHES: Just how long can a lightning discharge get? *Bulletin of the American Meteorological Society*, 101(1), E73–E86. <https://doi.org/10.1175/BAMS-D-19-0033.1>

MacGorman, D. R., Few, A. A., & Teer, T. L. (1981). Layered lightning activity. *Journal of Geophysical Research*, 86(C10), 9900–9910. <https://doi.org/10.1029/JC086iC10p09900>

Mansell, E. R., Macgorman, D. R., Ziegler, C. L., & Straka, J. M. (2002). Simulated three-dimensional branched lightning in a numerical thunderstorm model. *Journal of Geophysical Research*, 107(D9), 1–12. <https://doi.org/10.1029/2000JD000244>

Maragos, P., & Sun, F. K. (1993). Measuring the fractal dimension of signals: Morphological covers and iterative optimization. *IEEE Transactions on Signal Processing*, 41(1), 108. <https://doi.org/10.1109/tp.1993.193131>

Mareev, E. A., & Dementyeva, S. O. (2017). The role of turbulence in thunderstorm, snowstorm, and dust storm electrification. *Journal of Geophysical Research: Atmospheres*, 122, 6976–6988. <https://doi.org/10.1002/2016JD026150>

Mazur, V., & Rust, W. D. (1983). Lightning propagation and flash density in squall lines as determined with radar. *Journal of Geophysical Research*, 88(C2), 1495–1502. <https://doi.org/10.1029/JC088iC02p01495>

Nag, A., & Rakov, V. A. (2009). Some inferences on the role of lower positive charge region in facilitating different types of lightning. *Geophysical Research Letters*, 36(5), 126–127. <https://doi.org/10.1029/2008GL036783>

Niemeyer, L., Pietronero, L., & Wiesmann, H. J. (1984). Fractal dimension of dielectric breakdown. *Physical Review Letters*, 52(12), 1033–1036. <https://doi.org/10.1103/PhysRevLett.52.1033>

Petersen, D., Bailey, M., Beasley, W. H., & Hallett, J. (2008). A brief review of the problem of lightning initiation and a hypothesis of initial lightning leader formation. *Journal of Geophysical Research*, 113(D17), D17205. <https://doi.org/10.1029/2007JD009036>

Qie, X. (2005). The lower positive charge center and its effect on lightning discharges on the Tibetan Plateau. *Geophysical Research Letters*, 32(5), L05814. <https://doi.org/10.1029/2004GL022162>

Riousset, J. A., Pasko, V. P., Krehbiel, P. R., Thomas, R. J., & Rison, W. (2007). Three-dimensional fractal modeling of intracloud lightning discharge in a New Mexico thunderstorm and comparison with lightning mapping observations. *Journal of Geophysical Research*, 112, D15203. <https://doi.org/10.1029/2006JD007621>

Rison, W., Thomas, R. J., Krehbiel, P. R., Hamlin, T., & Harlin, J. (1999). A GPS-based three-dimensional lightning mapping system: Initial observations in central New Mexico. *Geophysical Research Letters*, 26(23), 3573–3576. <https://doi.org/10.1029/1999GL010856>

Sañudo, J., Gómez, J. B., Castaño, F., & Pacheco, A. F. (1995). Fractal dimension of lightning discharge. *Nonlinear Processes in Geophysics*, 2(2), 101–106. <https://doi.org/10.5194/npg-2-101-1995>

Scholten, O., Hare, B. M., Dwyer, J., Liu, N., Sterpka, C., Kolmasova, I., et al. (2021). A distinct negative leader propagation mode. *Scientific Reports*, 11(1), 16256. <https://doi.org/10.1038/s41598-021-95433-5>

Stock, M. G., Krehbiel, P. R., Lapierre, J., Wu, T., Stanley, M. A., & Edens, H. E. (2017). Fast positive breakdown in lightning. *Journal of Geophysical Research: Atmospheres*, 122, 8135–8152. <https://doi.org/10.1002/2016JD025909>

Stolzenburg, M., Rust, W. D., Smull, B. F., & Marshall, T. C. (1998). Electrical structure in thunderstorm convective regions: 1. Mesoscale convective systems. *Journal of Geophysical Research*, 103(D12), 14059–14078. <https://doi.org/10.1029/97JD03546>

Tan, Y., Tao, S., Liang, Z., & Zhu, B. (2014). Numerical study on relationship between lightning types and distribution of space charge and electric potential. *Journal of Geophysical Research: Atmospheres*, 119, 1003–1014. <https://doi.org/10.1002/2013JD019983>

Tan, Y., Tao, S., & Zhu, B. (2006). Fine-resolution simulation of the channel structures and propagation features of intracloud lightning. *Geophysical Research Letters*, 33(9), 499–505. <https://doi.org/10.1029/2005GL025523>

Tan, Y. B., Tao, S.-C., Zhu, B.-Y., Ma, M., & Lü, W.-T. (2007). A simulation of the effects of intra-cloud lightning discharges on the charges and electrostatic potential distributions in a thundercloud. *Chinese Journal of Geophysics*, 50(4), 916–930. <https://doi.org/10.1002/cjg2.1109>

Thomas, R. J., Krehbiel, P. R., Rison, W., Hunyady, S. J., Winn, W. P., Hamlin, T., & Harlin, J. (2004). Accuracy of the lightning mapping array. *Journal of Geophysical Research*, 109(14), D14207. <https://doi.org/10.1029/2004JD004549>

Tsonis, A. A. (1991). A fractal study of dielectric breakdown in the atmosphere. In D. Schertzer & S. Lovejoy (Eds.), *Non-linear variability in geophysics* (pp. 167–174). Springer.

Vecchi, G., La Ba Te, D., & Canavero, F. (1994). Fractal approach to lightning radiation on a tortuous channel. *Radio Science*, 29(4), 691–704. <https://doi.org/10.1029/93RS03030>

Williams, E. R., Cooke, C. M., & Wright, K. A. (1985). Electrical discharge propagation in and around space charge clouds. *Journal of Geophysical Research*, 90(D4), 6059–6070. <https://doi.org/10.1029/JD090iD04p06059>

Winn, W. P., Moore, C. B., & Holmes, C. R. (1981). Electric field structure in an active part of a small, isolated thundercloud. *Journal of Geophysical Research*, 86(C2), 1187–1193. <https://doi.org/10.1029/JC086iC02p01187>

Xu, D., Tan, Y., Zheng, T., Lin, H., Yu, J., Lei, Y., et al. (2021). Numerical simulation on the effects of the horizontal charge distribution on lightning types and behaviors. *Journal of Geophysical Research: Atmospheres*, 126(18), e2020JD034375. <https://doi.org/10.1029/2020JD034375>

Zhang, R., Zhang, G. S., Li, Y., Wang, Y. H., Wu, B., Yu, H., & Liu, Y. X. (2014). Estimate of NOX production in the lightning channel based on three-dimensional lightning locating system. *Science China Earth Sciences*, 57(7), 1613–1625. <https://doi.org/10.1007/s11430-013-4812-1>

Zheng, D., Wang, D., Zhang, Y., Wu, T., & Takagi, N. (2019). Charge regions indicated by LMA lightning flashes in Hokuriku's winter thunderstorms. *Journal of Geophysical Research: Atmospheres*, 124(13), 7179–7206. <https://doi.org/10.1029/2018JD030060>